Higher-Order Sliding Mode Control of Buck-Boost Converter fed Permanent Magnet DC Motor

Dhanasekar Ravikumar[1], Vijayaraja Loganathan[2], Ganesh Kumar Srinivasan[3] and Arman Salih Ahmad[4]

[1,2]Department of Electrical & Electronics Engineering, Sri Sairam Institute of Technology, West Tambaram, Chennai, Tamilnadu, India [3,4]Department of Electrical & Electronics Engineering, CEG campus, Anna University, Chennai, Tamilnadu, India
dhanasekar.eee@sairamit.edu.in (Corresponding author), vijayaraja.eee@sairamit.edu.in
ganeshkumar@annauniv.edu, armansalihahmad@gmail.com

Abstract: This paper presents the design and implementation of a second order sliding mode controller for a buck-boost converter fed PMDC machine. Two sliding surfaces, classical sliding surface, and PID sliding surface have been considered for controller design. The simulation of the designed controller has been carried out in Simulink with 490 Hz switching frequency for both no-load and changing load conditions. The hardware implementation is carried out using Arduino UNO controller for 490 Hz switching frequency. The performance of the classical sliding surface and PID sliding surface-based controllers has been compared in terms of steady-state error, overshoot, and settling time. The findings have been effectively obtained and presented, indicating the effectiveness of both controllers in terms of system stability and resilience to disturbances.

Keywords: converter; DC motor; proportional control; sliding mode control; variable speed drives

1. Introduction

Permanent Magnet DC (PMDC) motors are often the optimal choice for applications requiring motion control and power transmission due to their compact size and wide operating speed range. They can be used in place of gear motors in many applications, as they are capable of producing high torque at low speeds. This design offers several advantages, including maximum efficiency by eliminating field winding losses, compact size, and simpler control circuitry. PMDC motors find applications in a wide range of devices, from small toys and appliances to electric vehicles and industrial equipment [1]. They are especially suitable for adjustable speed and servo control applications where the motor operates at speeds under 5000 rpm. To control the speed and torque of these machines, a DC-DC converter such as a buck-boost converter can be used to regulate the voltage both in buck and boost mode applied to the machine's armature [2-4]. However, the nonlinear and uncertain nature of the system dynamics can make it challenging to design a control strategy that achieves the desired performance and robustness.

Sliding mode control is a well-established robust non-linear control technique that has been around for several decades. It is used in control systems that have uncertainties, disturbances, and nonlinear dynamics [5]. The conventional approach to sliding mode control has a drawback that requires implementation of a discontinuous control signal, which theoretically should switch with an infinite frequency to achieve complete rejection of uncertainty. The outcome of this situation is the occurrence of chattering phenomenon in the control variable, which can lead to both mechanical deterioration and noise, especially if the control variable is the speed of a motor. However, new advancements in the field have introduced higher order sliding mode control, which aims to provide a smoother control that incorporates the advantages of the conventional sliding mode control more precisely [6]. A homogeneity-based approach for developing HOSM controllers that are finite time convergent. This feature enables easy regularization of standard controllers which substantially improves their performance. This paper provides regularized equations design a second order sliding mode

Received: March 27th, 2025. Accepted: September 30th, 2025
DOI: 10.15676/ijeei.2025.17.3.11

controller [7]. In [8], the evolution of higher order sliding mode control from the mathematical problems that arose from the conventional sliding mode control and focuses on exploring the potential of high order sliding mode control as a replacement for conventional sliding mode control. The discussion also sets standard definitions for terms such as sliding mode order, relative degree and chattering attenuation. In [9], a second order sliding mode controller is designed for step down chopper fed dc drives which do not require current feedback. However, this controller is not regularized and may not be convergent on other converter fed DC drives. In [10], design and implement third order sliding mode controllers is proposed for a buck converter fed PMDC motor by homogeneity approach for Classical and PID sliding surfaces and provide a comparative analysis of their respective outcomes. Table 1 shows the survey of various sliding mode controller in recent situations based on the nature of load.

Table 1. Survey of various sliding mode controller in recent situations based on the nature of load

Reference number	Year	Converter type	Schemes in SMC	Nature of load	Problems addressed
[11]	2024	Inverter	Super twisting SMC	Permanent magnet synchronous motor	Changes in position of the rotor and speed
[12]	2024	Sepic converter	Second order SMC	PMDC motor	Speed control for various load torques
[13]	2024	Boost converter	Second order SMC	PMDC motor	Speed regulation for various load torques
[14]	2023	-	Integral sliding mode	DC motor	Track the reference speed
[15]	2023	Full bridge buck inverter	Sensorless SMC	DC motor	DC motor control under renewable source of energy
[16]	2022	Full bridge inverter	Washout filter based SMC	PMDC motor	Speed tracking
[17]	2024	Modified negative output Luo converter	Fuzzy sliding mode	Resistive load (R-Load)	Low ripple and steady state output
[18]	2024	Differential Boost inverter	sliding mode control	R-Load	Robustness in supply voltage and load variations
[19]	2024	Buck converter	Non singular fast terminal sliding mode	R-Load	Accuracy in tracking the voltage under disturbances
[20]	2024	Buck converter	Fuzzy neural network sliding mode	R-Load	Voltage tracking without chattering
[21]	2024	Sepic converter	Embedded sliding mode	R-Load	Regulation of output voltage
[22]	2023	Two level inverter	Fractional order Sliding mode control	Induction motor	Torque ripple reduction
[23]	2022	Direct matrix converter	Sliding mode control	Induction motor	Chattering reduction
[24]	2024	DC-DC converter	Barrier function based adaptive sliding mode	Electric vehicle	Robust in uncertainties and provides system safety
[25]	2024	Improve single phase Z source inverter	Fractional order sliding mode	Grid	Regulates active power, reactive power, voltage, frequency and harmonics

From the above it can be seen that implementation of Higher Order Sliding Mode Controller (HOSMC) for Buck-Boost converter fed PMDC motor is challenging.
The key contributions and novelty of this paper are summarized as follows,

- A second-order sliding mode controller integrating proportional-integral-derivative (PID) and classical sliding surfaces are designed for a buck-boost converter coupled with a PMDC motor to examine servo and regulatory responses..
- The proposed control law exhibits robustness to system uncertainties, efficiently reduces overshoot, rejects disturbances, and guarantees adequate control quality across a broad operating range.
- The effectiveness of the suggested design and control strategies has been validated through hardware implementation and experimental results.

The paper is formulated as follows, section 2 explains the modeling of PMDC motor with buck-boost converter, section 3 describes the controller design, section 4 discuss the simulation results, section 5 explains the hardware section and section 6 discuss the conclusion.

2. Modeling of PMDC Motor Powered by Buck-Boost Converter

The block diagram of Buck-Boost converter fed PMDC motor illustrating the flow of power signal and control signal has been presented in Fig.1. It consists of DC source, buck-boost converter that regulates the output voltage supplied to the DC machine, PMDC machine, PWM gate driver and control system. The control system i.e., a second order sliding mode controller regulates the output voltage of the buck-boost converter based on the desired speed and torque of the DC machine. The regularized equations provided in [1] have been used to construct second order sliding mode controller for two sliding surfaces namely Classical Sliding Surface (CSS) and PID Sliding Surface (PIDSS).

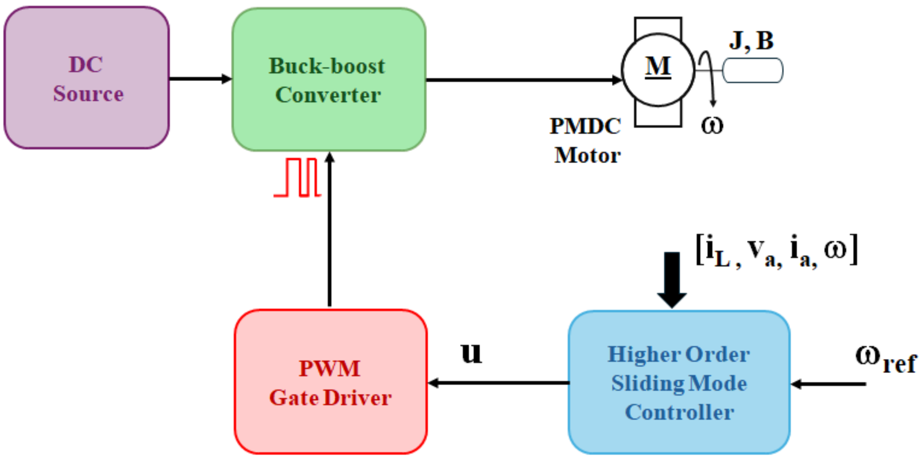

Figure 1. Block Diagram of Buck-Boost converter fed PMDC motor

The circuit diagram shown in Fig.2 explains the implementation of HOSMC for buck-boost converter fed PMDC motor.
The components in the system are:
E – Source voltage (V)
S – Converter switch (IGBT)
D – Diode
L – Inductance of the converter (H)
C – Capacitance of the converter (F)
R_a – Armature resistance (Ω)

La – Armature inductance (H)
M – Motor
J – Moment of inertia of shaft (kg m^2)
B – Viscous friction coefficient (Nm/rad)
V_a – Armature voltage (volts)
i_L – Inductor current (Ampere)
i_a – Armature current (Ampere)

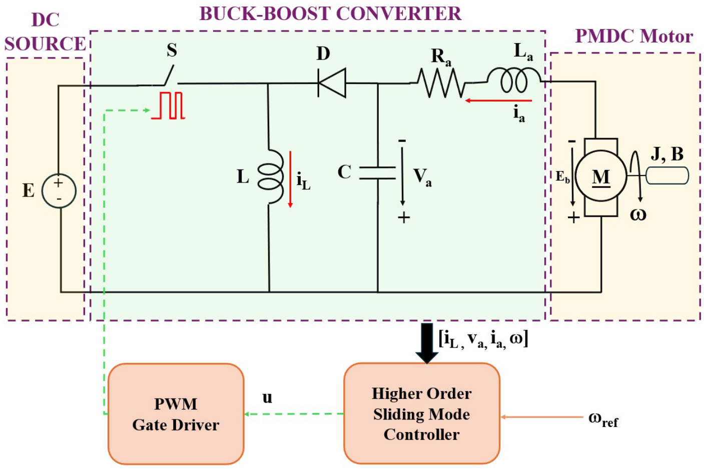

Figure 2. Circuit diagram of Buck-Boost converter with PMDC motor

The state equations so obtained are presented from (1) to (4).

$$\frac{di_L}{dt} = \frac{-(1-u)}{L} v_a + u\frac{E}{L} \tag{1}$$

$$\frac{dv_a}{dt} = \frac{(1-u)}{C} i_L - \frac{i_a}{C} \tag{2}$$

$$\frac{di_a}{dt} = \frac{v_a}{L_a} - \frac{R_a i_a}{L_a} - \frac{k\omega}{L_a} \tag{3}$$

$$\frac{d\omega}{dt} = \frac{k}{J} i_a - \frac{B}{J}\omega - \frac{T_L}{J} \tag{4}$$

3. Controller Design

Originating from the 1960s in the former Soviet Union, sliding mode control is a non-linear control strategy for Variable Structure Systems (VSS).VSS are systems that intentionally alter their physical structure or network topology during the transient phase according to a predetermined structure control law. VSS can yield system characteristics that differ significantly from the properties of the individual substructures by sliding mode control. Thus, two sub-structures that are both asymptotically stable can make up an asymptotically stable system. Sliding surface is nothing but a mathematical equation defined in the error phase plane. The objective of sliding mode control is to drive the system state towards the desirable region and keep it there. The sliding surface is designed in such a way that the system state slides along it, meaning that the system state remains on the sliding surface during the entire operation of the control system. The sliding surface is defined using a set of control parameters that are selected to ensure that the system state follows a desired trajectory. To get rid of chattering, Higher Order Sliding Mode (HOSM) is introduced as a replacement to traditional sliding mode control.

A. Relative Degree calculation of Buck-Boost converter fed PMDC Motor

The labels declared in (4) to (9) have been used for ease of algebraic operations.

$$a_1 = \frac{-1}{L}; a_2 = \frac{-1}{C}; a_3 = \frac{1}{C}; a_4 = \frac{1}{La}; \; a_5 = -\frac{R_a}{L_a};$$

$$a_6 = \frac{-k_e}{La}; a_6 = \frac{kt}{J}; \; a_8 = \frac{-B}{J}; a_9 = \frac{-1}{J}$$

$$x_1 = a_7 a_5 + a_7 a_8; \; x_2 = a_7 a_4 \quad (5)$$

$$x_3 = a_7 a_6 + a_8^2; \; x_4 = a_8 a_9 \quad (6)$$

$$z_1 = x_2 a_3; \;\; z_2 = x_1 a_5 + x_2 a_2 + x_3 a_7 \quad (7)$$

$$z_3 = x_1 a_4; \;\; z_4 = x_1 a_6 + x_3 a_8 \quad (8)$$

$$z_5 = x_3 a_9 \quad (9)$$

Rewriting the state equations with these labels, Equations (10) to (13) are obtained.

$$\frac{di_L}{dt} = -a_1(1-u)v_a + a_1 uE \quad (10)$$

$$\frac{dv_a}{dt} = a_3(1-u)i_L + a_2 i_a \quad (11)$$

$$\frac{di_a}{dt} = a_4 v_a + a_5 i_a + a_6 \omega \quad (12)$$

$$\frac{d\omega}{dt} = a_7 i_a + a_8 \omega + a_9 T_L \quad (13)$$

The error signal and its derivatives are obtained and presented in Equations (14) to (17).

$$e = \omega_r - \omega \quad (14)$$

$$\dot{e} = -\dot{\omega} = -(a_7 i_a + a_8 \omega + a_9 T_L) \quad (15)$$

$$\ddot{e} = -\ddot{\omega} = -(x_1 i_a + x_2 v_a + x_3 \omega + x_4 T_L) \quad (16)$$

$$\dddot{e} = -\dddot{\omega} = -(z_1 i_L + z_2 i_a + z_3 v_a + z_4 \omega + z_5 T_L \; - u z_1 i_L) \quad (17)$$

The control term 'u' appears in the third derivative of error signal. That is, the error signal becomes discontinuous at the third time derivative and hence its relative degree $d = 3$. For PIDSS and CSS the order of the controller for the buck-boost converter fed PMDC motor is $r = d - 1$ and this is presented in the next section.

B. Calculation of order of controller for the sliding surfaces

The objective of the paper is to evaluate the performance of the controller for Classical and PID sliding surfaces. Classical sliding surface is given in (18).

$$\sigma = ce + \dot{e} \quad (18)$$

Where c is the slope of the sliding trajectory in the phase plane.

To find the order of the controller, differentiate the sliding surface with respect to time until uncertainty arises as shown in (19) and (20).

$$\dot{\sigma} = c\dot{e} + \ddot{e} \quad (19)$$

$$\ddot{\sigma} = c\ddot{e} + \dddot{e} \quad (20)$$

The PID sliding surface is defined in (21)

$$\sigma = Pe + I\int edt + D\dot{e} \quad (21)$$

The sliding surface includes the error signal, derivative and it's integral. By inclusion of the integral in the sliding surface, reaching phase is very quick in $e, \dot{e}$ plane. P, I, D are the tuning parameters that set the sliding trajectory.

To find the order of the controller 'r', differentiate with respect to time until uncertainty arises as shown in (22) and (23).

$$\dot{\sigma} = P\dot{e} + Ie + D\ddot{e} \quad (22)$$

$$\ddot{\sigma} = P\ddot{e} + I\dot{e} + D\dddot{e} \quad (23)$$

The error $\ddot{e}$ is discontinuous and has a *u* term in it. The uncertainty '*u*' arises in the second time derivative of the sliding surface. Thus, for PIDSS also $r = 2$.

C. Construction of classical sliding surface for Buck-Boost converter fed PMDC Motor

The sliding surfaces are further expanded in terms of the state variables and the equivalent control signal is calculated in this section. The conventional sliding surface and its derivatives are constructed as shown below.

From (44), the CSS is defined as

$$\sigma = ce + \dot{e} \quad (24)$$

Substituting (14) and (15) in (24), we get

$$\sigma = c(\omega_r - \omega) - a_7 i_a - a_8\omega - a_9 T_L \quad (25)$$

$$\sigma = c\omega_r - a_7 i_a - (c + a_8)\omega - a_9 T_L \quad (26)$$

Consider label given in (27) for further algebraic operations.

$$z = c + a_8 \quad (27)$$

The CSS is now given in (28)

$$\sigma = c\omega_r - a_7 i_a - z\omega - a_9 T_L \quad (28)$$

On differentiating with respect to time, (28) is obtained. ω_r and T_L are constants and hence yield 0 on differentiation.

$$\dot{\sigma} = -a_7 \dot{i_a} - z\dot{\omega} \quad (29)$$

Substituting (12) and (13) in (29), we get (30)

$$\dot{\sigma} = z_1 i_a + z_2\omega + z_3 T_L + z_4 v_a \quad (30)$$

The coefficients used are listed in (31) to (34)

$$z_1 = za_7 + a_7 a_5 \quad (31)$$

$$z_2 = za_8 + a_7 a_6 \quad (32)$$

$$z_3 = za_9 \quad (33)$$

$$z_4 = -a_7 a_4 \quad (34)$$

On further differentiating, we get (35)

$$\ddot{\sigma} = z_1 i_a + z_2\dot{\omega} + z_4\dot{v}_a \quad (35)$$

On substituting Equations (31), (32) and (34) in (35), (36) is obtained.

$$\ddot{\sigma} = x_1 i_L + x_2 i_a + x_3 v_a + x_4\omega + x_5 T_L - ux_1 i_L) \quad (36)$$

The coefficients used are listed in (37) to (41)

$$x_1 = z_4 a_3 \quad (37)$$

$$x_2 = z_1 a_5 + z_2 a_7 + z_4 a_2 \quad (38)$$

$$x_3 = z_1 a_4 \quad (39)$$

$$x_4 = z_1 a_6 + z_2 a_8 \quad (40)$$

$$x_5 = z_2 a_9 \quad (41)$$

Set $\ddot{\sigma} = 0$ to obtain the equivalent control signal 'u_{eq}' as shown in (42)

$$u_{eq} = \frac{x_1 i_L + x_2 i_a + x_3 v_a + x_4\omega + x_5 T_L}{x_1 i_L} \quad (42)$$

The function of this equivalent control signal is to produce motion of the Representative Point (RP) in the phase plane. The calculated signals σ and $\dot{\sigma}$ are fed as inputs to the second order controller and simulated in section 4.

D. Construction of PID sliding surface for Buck-Boost converter fed PMDC Motor

The conventional sliding surface and its derivatives are constructed as shown below. From (43), the PIDSS is defined as

$$\sigma = Pe + I\int e\,dt + D\dot{e} \quad (43)$$

Substituting (14) and (15) in (43), we get

$$\sigma = P(\omega_r - \omega) + I\int(\omega_r - \omega)dt + -D(a_7 i_a + a_8\omega + a_9 T_L) \quad (44)$$

$$\sigma = P\omega_r + I\int(\omega_r - \omega)dt - Da_7 i_a - a_9 T_L - \omega(Da_8 + P) \quad (45)$$

Consider label given in (46) for further algebraic operations.

$$z = Da_8 + P \quad (46)$$

$$\sigma = P\omega_r + I\int(\omega_r - \omega)dt - Da_7 i_a - a_9 T_L - z\omega \quad (47)$$

On differentiating the sliding surface, (48) is obtained.

$$\dot{\sigma} = \mathrm{P\dot{e} + Ie + D\ddot{e}} \tag{48}$$

Substituting (14), (15) and (16) in (48), (49) is obtained.

$$\dot{\sigma} = -\mathrm{P}(a_7 i_a + a_8 \omega + a_9 T_L) + \mathrm{I}(\omega_r - \omega) - \mathrm{D}(x_1 i_a + x_2 v_a + x_3 \omega + x_4 T_L) \tag{49}$$

On rearranging, Equations (50) and (51) are obtained.

$$\dot{\sigma} = -(\mathrm{P}a_7 + \mathrm{D}x_1) i_a - (\mathrm{P}a_8 + \mathrm{I} + \mathrm{D}x_3)\omega - (\mathrm{D}x_2) v_a - (\mathrm{P}a_9 + \mathrm{D}x_4) T_L + \mathrm{I}\omega_r \tag{50}$$

$$\dot{\sigma} = z_1 i_a + z_2 \omega + z_3 v_a + z_4 T_L + I\omega_r \tag{51}$$

The coefficients used are listed from (52) to (55)

$$z_1 = -(Pa_7 + Dx_1) \tag{52}$$

$$z_2 = -(Pa_8 + I + Dx_3) \tag{53}$$

$$z_3 = -(Dx_2) \tag{54}$$

$$z_4 = -(Pa_9 + Dx_4) \tag{55}$$

On further differentiating the sliding surface, (56) is obtained.

$$\ddot{\sigma} = z_1 i_a + z_2 \dot{\omega} + z_3 \dot{v}_a \tag{56}$$

On substituting (31), (32) and (33) in (78), (57) is obtained.

$$\ddot{\sigma} = z_1(a_4 v_a + a_5 i_a + a_6 \omega) + z_2(a_7 i_a + a_8 \omega + a_9 T_L) + z_3(a_3(1-u) i_L + a_2 i_a) \tag{57}$$

On rearranging, (58) and (59) are obtained.

$$\ddot{\sigma} = (z_1 a_5 + z_2 a_7 + z_3 a_2) i_a + (z_1 a_6 + z_2 a_8)\omega + (z_1 a_4) v_a + (z_2 a_9) T_L + (z_3 a_3) i_L - u(z_3 a_3) i_L \tag{58}$$

$$\ddot{\sigma} = x_1 i_a + x_2 \omega + x_3 v_a + x_4 T_L + x_5 i_L - u x_5 i_L \tag{59}$$

Set $\ddot{\sigma} = 0$ to obtain the equivalent control signal 'u_{eq}' as shown in (60)

$$u_{eq} = \frac{x_1 i_a + x_2 \omega + x_3 v_a + x_4 T_L + x_5 i_L}{x_5 i_L} \tag{60}$$

The calculated signals σ and $\dot{\sigma}$ are fed as inputs to the second order controller and simulated in section 4.

E. Construction of second order sliding mode controller

The sliding surface $'\sigma'$ is a mathematical construct defined by the designer. The r^{th} derivative of the sliding surface is given by (61).

$$\sigma^{(r)} = h(t,x) + g(t,x)u, g = \frac{\partial}{\partial u}\sigma^{(r)} \neq 0 \tag{61}$$

'*h*' and '*g*' are unknown smooth functions.

In [1],Arie Levant proposes homogeneity-based approach for developing HOSM controllers that are finite time convergent. This feature enables regularization of standard controllers for different '*r*'.

The condition for constructing the HOSMC proposed in [1] is that the inequalities in (62) hold for Equation (63).

$$0 < K_m \leq \frac{\partial}{\partial u}\sigma^{(r)} \leq K_M, \left|\sigma^{(r)}\right|_{u=0} \leq C \tag{62}$$

$$K_m, K_M, C > 0 \tag{63}$$

The regularized controller of order '*r*' can be constructed from (64) to (70).

$$u = -\alpha\psi_{r-1,r}\left(\sigma, \dot{\sigma}, \dots, \sigma^{(r-1)}\right) \tag{64}$$

Where,

$$\psi_{(0,r)} = \mathrm{sign}(\sigma) \tag{65}$$

$$\text{Let } i = 1,2,\dots,r-1 \tag{66}$$

$$\psi_{i,r} = \mathrm{sat}\left(\frac{[\sigma^{(i)} + \beta_i N_{i,r}\psi_{i-1,r}]}{N_r^{r-i}}, \varepsilon_i\right) \tag{67}$$

$$\text{and } N_{i,r} = \left(|\sigma|^{\frac{q}{r}} + |\dot{\sigma}|^{\frac{q}{r-1}} + \dots + \left|\sigma^{(i-1)}\right|^{\frac{q}{r-i+1}}\right)^{\frac{r-i}{q}} \tag{68}$$

$$N_r = \left(|\sigma|^{\frac{q}{r}} + |\dot{\sigma}|^{\frac{q}{r-1}} + \dots + \left|\sigma^{(r-1)}\right|^{q}\right)^{\frac{1}{q}} \tag{69}$$

Where q is the LCM of 1, 2, …, r.
And the saturation function is given as

$$\text{sat}(z, \varepsilon_i) = \min\left(1, max\left(-\frac{z}{\varepsilon_i}\right)\right) \tag{70}$$

$\alpha, \beta_i > 0$ are the tuning parameters of the HOSMC.
From this, 'i' and 'q' are calculated as $i = 1$ and $q = 2$.
For the calculated r, i and q, the second order controller is constructed and presented in (71).

$$u_{sw} = -\alpha\ sat\left(\frac{\left[\dot{\sigma}+\beta(|\sigma|+|\dot{\sigma}|^2)^{\frac{1}{2}}\ sign(\sigma)\right]}{(|\sigma|+|\dot{\sigma}|^2)^{\frac{1}{2}}}, \varepsilon\right) \tag{71}$$

The control signal to be fed to the PWM gate driver is given as (72)

$$u = u_{sw} + u_{eq} \tag{72}$$

However, the inequality condition as mentioned in Equations (62) and (63) is not satisfied for both the sliding surfaces which causes u_{sw} to turn negative. This can be rectified by inverting the sign of u to as illustrated in (73)

$$u = -(u_{sw} + u_{eq}) \tag{73}$$

The function of the equivalent control signal can be described as generating or creating movement within the phase portrait of a system. This signal plays a crucial role in the control process, as it determines the direction and speed of the motion of the system's state trajectory. In conventional sliding mode control, order of the sliding surface is mandatorily made equal to 1 as mentioned in [2]. The impact of both CSS and PIDSS on the control signal is illustrated in section 4 respectively.

4. Simulation Results and Discussions

This section details the results of MATLAB/SIMULINK simulation of Second Order Sliding Mode Control of Buck-Boost converter fed PMDC motor operating under changing loads for 490 Hz switching frequency. Feedback variables used for the closed loop operation of higher order sliding mode control algorithms are inductor current 'iL', armature voltage 'Va', armature current 'ia' and speed 'ω' are taken as feedback. The simulation outputs and associated parameters of the sliding mode control strategy are presented and analyzed for both CSS and PIDSS in this section. The specifications of the PMDC motor and converter considered for simulation is given in Table 2 and Table 3.

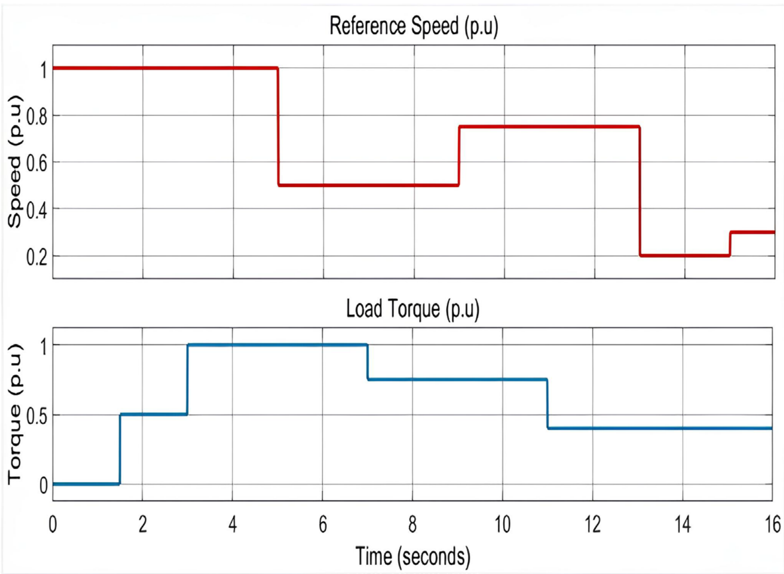

Figure 3. Reference Speed and Load Torque

The PMDC motor must track the reference speed for the varying load torque which is shown in Fig. 3.

Table 2. Motor Specifications

Motor parameter	Value
Power, P_o	18 W
Voltage, V_a	12 V
Current, I_a	1.5 A
Armature Resistance,	2.6 Ω
Armature Inductance,	712.85 mH
Back emf constant, k_e	0.0522 V s/rad
Moment of inertia, J	8.86138 x 10^{-5} kg m2
Viscous friction	1.647 x 10^{-4} Nm/rad
Speed, ω	157 rad/s

Table 3. Converter Specifications

Converter parameter	Value
Input Voltage, E	9 V
Frequency, f_s	490 Hz
Inductance, L	1.5 mH
Capacitance, C	1000 μF
Switch	IGBT

A. Classical sliding surface

The second order SMC is simulated for the converter designed for 490 Hz. The slope of the sliding surface is set to be 16 for quick rise time. The sliding surface is given by (74).

$$\sigma = ce + \dot{e} \tag{74}$$

where $c = 16$ The other tuning parameters were tuned to the following values by trial and error [26] and presented in (75)

$$\beta = 2; \quad \varepsilon = 1; \quad \alpha = 0.58 \tag{75}$$

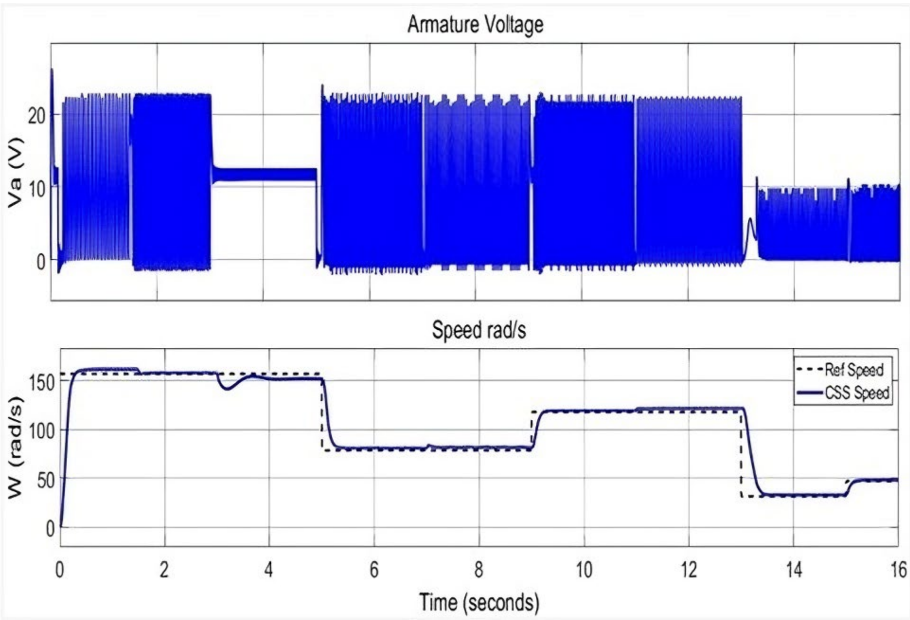

Figure 4. Armature Voltage and speed of CSS SMC

The cause for the presence of oscillations in armature voltage as shown in Fig.4 is due to the insufficiency of tuning parameters of the sliding surface. This can be visualized with the help of a phase portrait.

B. PID Sliding Surface

The main limitation of the CSS is its trajectories rigidity. This drawback can be overcome by PIDSS which has a flexible sliding surface. The advantages of PIDSS can be visualized with the simulation results. The sliding surface is given by (76)

$$\sigma = Pe + I\int edt + D\dot{e} \tag{76}$$

PID tuning was performed by Ziegler Nichols method. The simulation was performed with parameters defined in Equation (77)

$$P = 1.05;\quad I = 12;\quad D = 0.0024 \tag{77}$$

The functions of β and ε were explained in the previous section. By trial and error method the values of β and ε were tuned to obtain better control of magnitude of jumps in u.

$$\alpha = 0.58;\ \beta = 1; \varepsilon = 2 \tag{78}$$

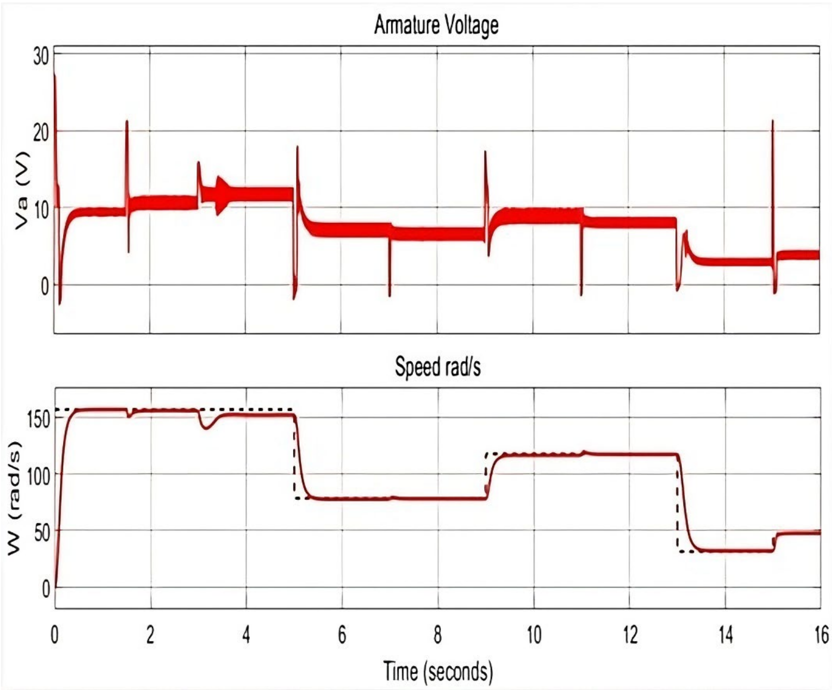

Figure 5. Armature voltage and speed of PIDSS SMC

The simulation result in Fig.5 shows that the voltage ripple has been significantly reduced with the maximum ripple being 2V. This has been achieved due to the flexibility of the sliding surface and the effect it has on the magnitude of the quasi-continuous state of switching signal u.

C. Comparative Analysis and Inference

The second order SMC for the Buck-Boost converter fed PMDC has been designed and simulated for CSS and PIDSS at 490 Hz and information about the control signals have been obtained in this section. The performance of both surfaces is analysed in this section for changes in constant load torque.

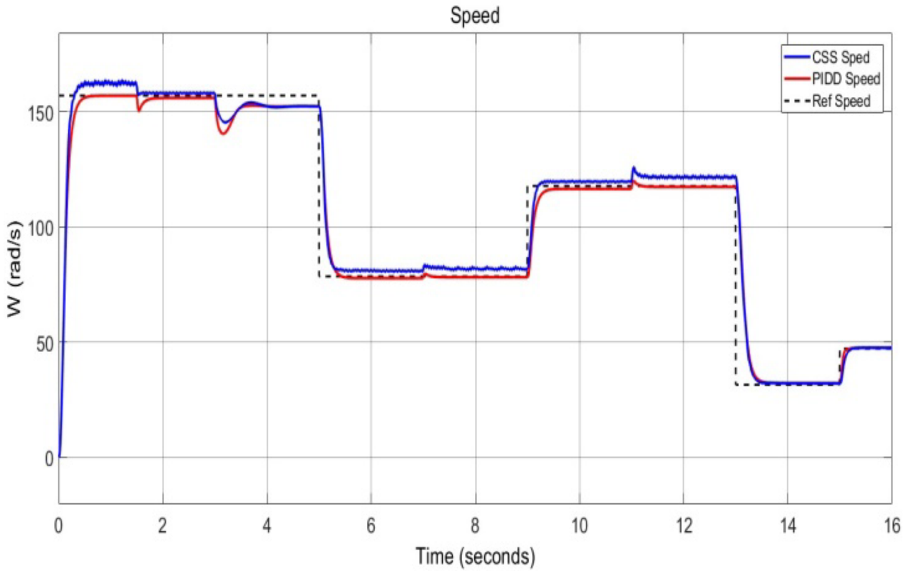

Figure 6. Speed response comparison

Table 4. Speed response comparison (Simulation study)

Time in seconds	Ref Speed (p.u)	Load Torque (p.u)	Settling time (seconds)		Error %	
			CSS	PIDSS	CSS	PIDSS
0-1.5	1	0	0.505	0.5	-4	0.6
1.5-3	1	0.5	0.122	0.2	-0.94	0.84
3-5	1	1	0.463	0.433	2.78	2.764
5-7	0.5	1	0.3	0.498	-4.2	0.7
7-9	0.5	0.75	0.052	0.15	-4.3	0.17
9-11	0.75	0.75	0.2	0.313	-1.14	1.297
11-13	0.75	0.4	0.154	0.164	-3.89	0.26
13-15	0.2	0.4	0.506	0.6	-2.92	-2.32
15-16	0.3	0.4	0.251	0.563	-0.848	-0.72

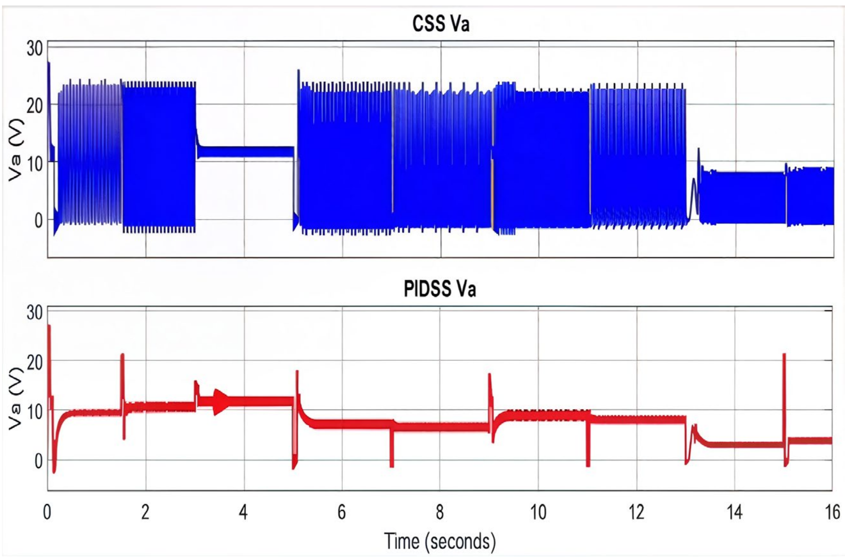

Figure 7. Armature voltage comparison

The speed responses and speed error of both CSS and PIDSS second order SMCs have been compared and presented in Fig.6. It can be seen that the speed of CSS second order SMC has comparatively poor response to changes in reference speed whereas the response of PIDSS second order SMC is balanced for both the changes in reference speed as well as changes in load torque. The reason behind this observation is explained further into the analysis. Table 4 and Fig.12 make it evident that the speed of CSS second order SMC has comparatively poor response to changes in reference speed but handles change in load torque well whereas the response of PIDSS second order SMC is balanced for both the changes in reference speed as well as changes in load torque.

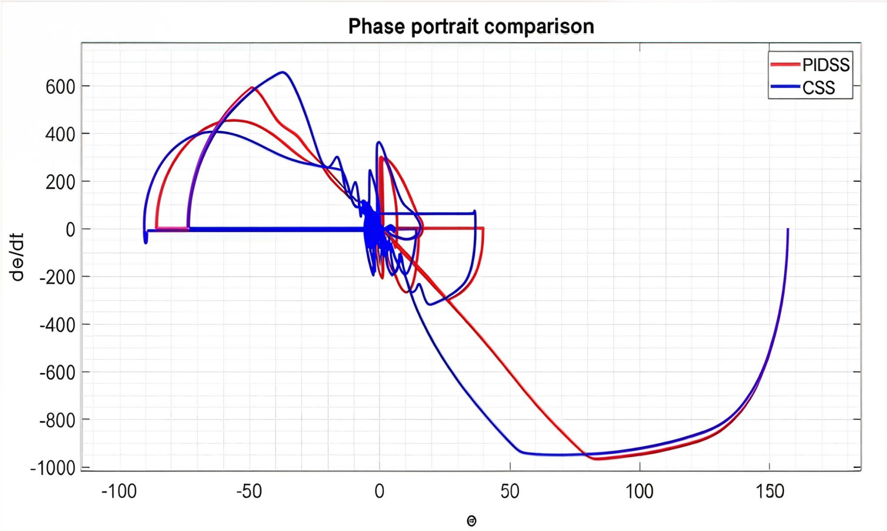

Figure 8. Phase portrait comparison

As shown in Fig.7, the armature voltage has very low ripple content in PIDSS SMC response which makes the response to change in reference speed to be smooth. The PIDSS can be made more flexible by tuning PID values and the controller can be made to provide smooth control signal by adjusting β and ε. In other words, rigidity of both the sliding surface and controller can be adjusted in PIDSSSMC to obtain balanced response for speed and torque changes. This feature is absent in CSS SMC. Even if the controller rigidity is adjusted the rigidity of the sliding surfaces causes the jumps to be of high magnitude in the control signal and hence the speed response of CSS SMC is always relatively poor for changes in reference speed signal. The phase portrait comparison in Fig.8 shows that PIDSS is a smooth curve in all regions whereas the CSS is a rigid fixed line. Also, the chattering phenomenon as mentioned earlier is evident in CSS. For a high change in reference speed the PIDSS SMC RP traverses from II quadrant to I quadrant and then onto the sliding surface. This implies that the error has changed sign and speed response is lagging.

According to the simulation study, classical sliding surface based SMCs have comparatively sluggish settling periods even if they track control variables with an acceptable degree of accuracy in various applications. This can be overcome by PID sliding surface which can be tuned to operate in optimum state which provides better tracking accuracy.

5. Experimental Implementation and Performance Discussions

This section presents the results of the hardware implementation of Second Order Sliding Mode Control (SMC) for a Buck-Boost converter fed PMDC motor operating under no-load at a switching frequency of 490 Hz. The hardware results are presented and analysed for both Classical Sliding Surface (CSS) and Proportional Integral Derivative Sliding Surface (PIDSS). Table 6 presented the list of components in hardware. The hardware implementation is illustrated in Fig.9, with a basic block diagram consisting of an RPS, Buck- Boost converter, TLP250 driver circuit, and Arduino UNO controller.

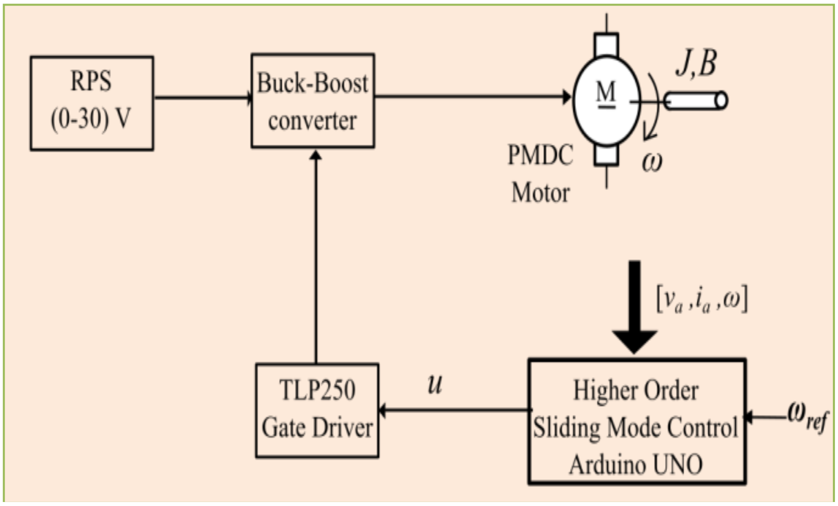

Figure 9. Hardware block diagram

Table 6. Component list

Components	Specifications
IGBT	15N120NDS
Driver Circuit	TLP250
Diode	RHRP3060
Inductor	1.5 mH
Capacitor	1000 µF
Controller	Arduino UNO
Voltage Sensor	A7840
Current Sensor	HE055T01
Speed Sensor	IR encoder + TC4584BP
PMDC motor	18 W, 12V, 1500 rpm
Step down	(230/18) V ,(230/9) V
Voltage regulator	LT915CP
Bridge rectifier	MB3510

The RPS maintains a constant 9 V voltage across its terminals. The power from the RPS is modulated through a buck-boost converter to power the PMDC motor. Feedback signals, which include the motor's armature voltage, current, and speed, are sent to the Arduino UNO controller. The Arduino UNO is programmed with second-order sliding mode control to generate a 490 Hz PWM signal which aims to regulate the motor speed to match the desired reference speed. The PWM signal is amplified from 5V to 15V using the TLP250 driver circuit before being supplied to the IGBT switch.

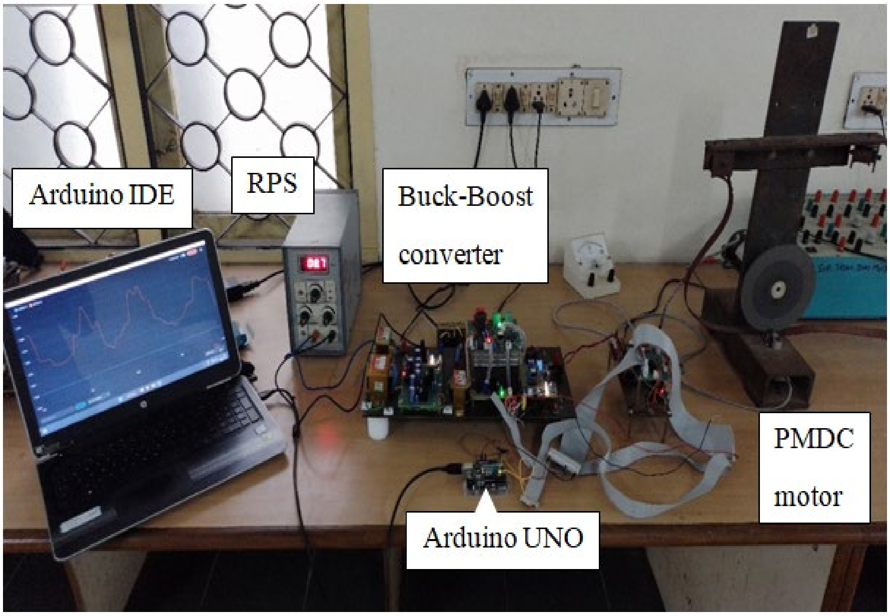

Figure 10. HOSMC Buck-Boost converter fed PMDC drive

Step down transformers are employed to reduce the voltage from the 230 V single-phase supply to 18 V and 9 V. The output is then converted to DC using diode bridge rectifiers. Capacitors of 1000 µF are used to eliminate the ripple content, resulting in a clean DC signal of 15 V and 5 V, which are used for biasing the sensors and gate driver. The board comes with various input and output pins that allow users to connect and control a wide range of sensors, actuators, and other electronic components. The complete HOSMC PMDC Buck-Boost converter fed PMDC drive has been portrayed in Fig.10. The Serial Plotter feature of Arduino IDE has been used to plot real time data of reference and actual speed of the motor in RPM. The speed, voltage, and current signals were exported in .csv format using the Serial print feature and subsequently plotted in MATLAB.

A. Comparative Analysis and Inference

The CSS HOSMC was implemented with the following tuning parameters

$C = 16, \alpha = 0.61,\ \beta = 2,\ \varepsilon\ = 1$

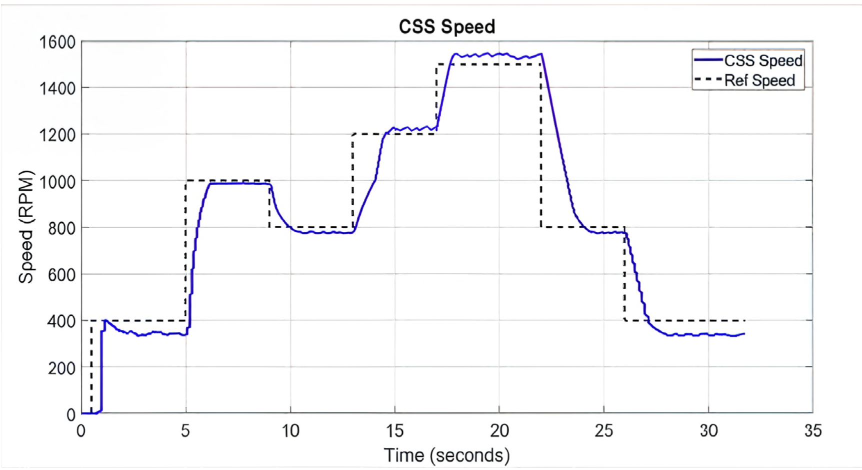

Figure 11. Speed response of CSS SMC

The speed response presented in Fig.11 indicates that the controller has achieved the desired speed regulation of the PMDC motor but with considerable steady state error.

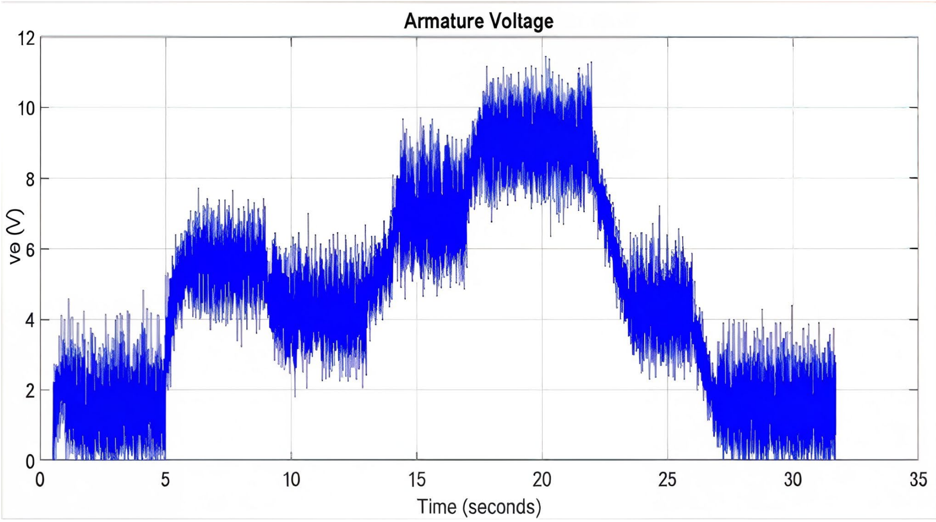

Figure 12.Armature voltage for CSS SMC

The magnitude of discontinuous jumps in the control signal on the sliding surface is maximum and this is due to the rigidity of the classical sliding surface. A curved sliding surface or a closed sliding surface will result in the control signal having low magnitude of discontinuous jumps. The armature voltage of the PMDC motor has been presented in Fig.12.

B. PID Sliding Surface SMC

PIDSS HOSMC was implemented with the following tuning parameters
P = 0.73, I = 60, D = 0.0025, $\alpha = 0.61$, $\beta = 1$, $\varepsilon = 2$

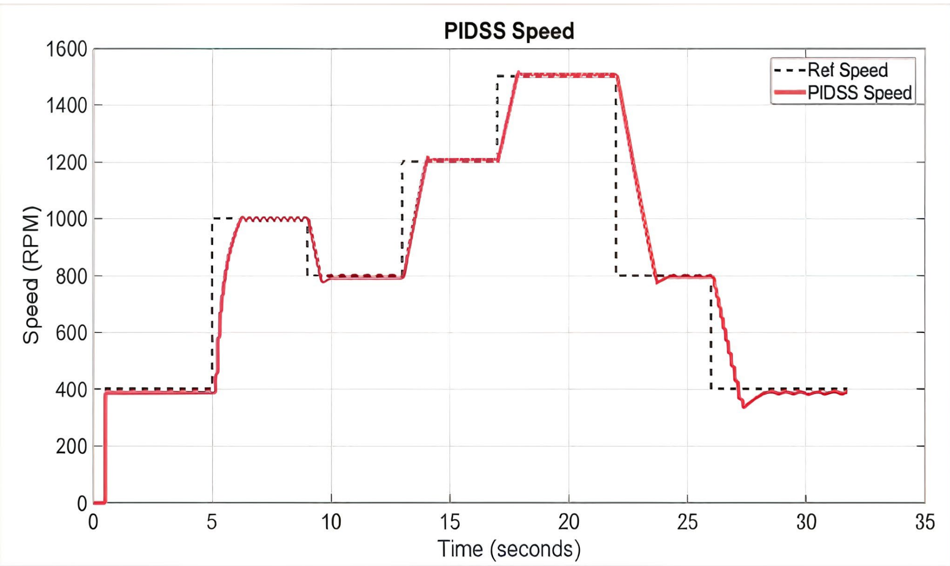

Figure 13.Speed response of PIDSS SMC

The speed response presented in Fig.13 shows the control signal generation of PIDSS sliding surface indicates that the controller has effectively achieved the desired speed regulation of the PMDC motor. The magnitude and frequency of discontinuous jumps in the control signal on the sliding surface is well controlled in PID sliding surface than the linear Classical sliding surface.

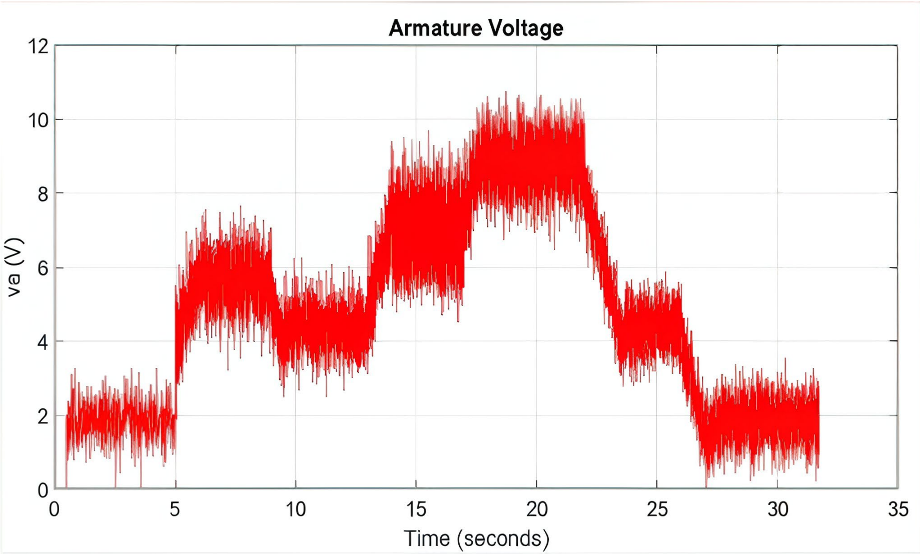

Figure 14. Armature voltage for PIDSS SMC

The armature voltage of the PMDC motor has been presented in Fig.14. The motor operates in both continuous and discontinuous current modes under no-load condition.

C. CSS AND PIDSS HOSMC COMPARISON

The speed regulation of both CSS and PIDSS HOSMC have been plotted and compared in Fig.15 and Fig.16. Comparing PIDSS with CSS HOSMC, it is evident that PIDSS exhibits a faster settling time and nearly 0% steady-state error, whereas CSS HOSMC shows a considerable margin of error.

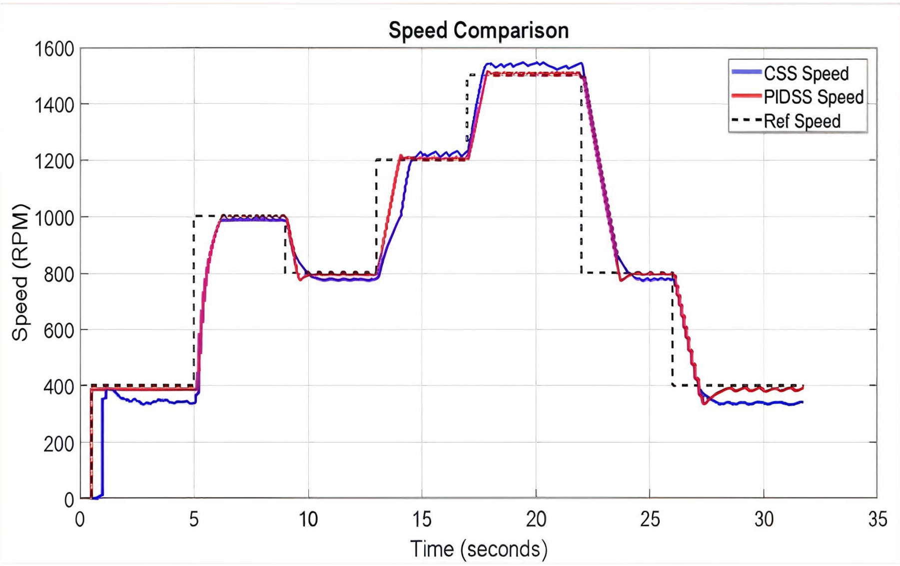

Figure 15. Speed regulation curve

The PIDSS HOSMC has faster settling time for both positive and negative change in reference speed than the CSS HOSMC. As mentioned earlier, the inclusion of integral of error term makes the PID sliding surface a smooth curve in comparison to the rigid and linear CSS sliding surface. Therefore, the driving of RP onto the sliding surface is quick in PIDSS than CSS and hence the faster settling time.

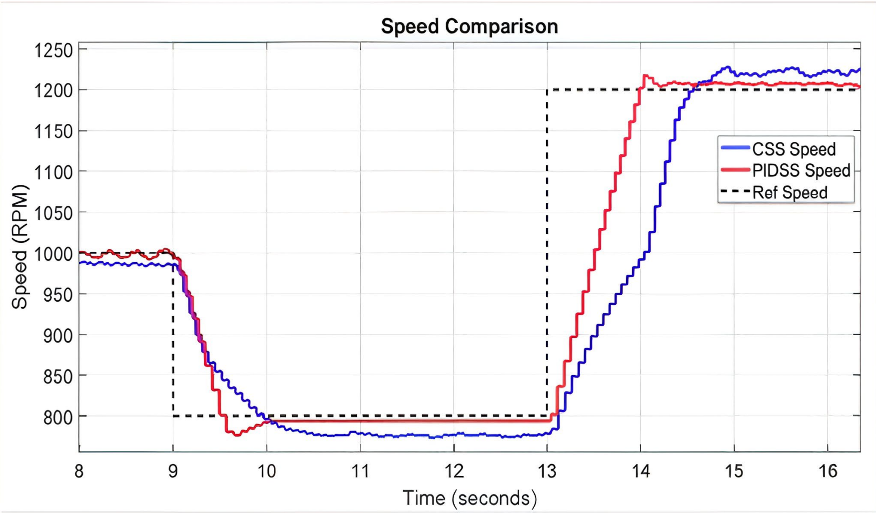

Figure 16. Speed regulation comparison

From the figure, it can be observed that the magnitude and frequency of discontinuous jumps in the control signal on the sliding surface is well controlled in PID sliding surface than the linear Classical sliding surface.

Table 7. Speed response comparison in practical setup

Time in seconds	Ref Speed (RPM)	Settling time		Error %	
		CSS	PIDSS	CSS	PIDSS
0-0.5	0	-	-	0	0
0.5-5	400	-	-	15.022	2.95
5-9	1000	2.95	2.96	1.088	-0.17
9-13	800	1.17	0.7	2.94	0.72
13-17	1200	1.57	1.02	-2	-0.62
17-22	1500	0.78	0.84	-2.84	-0.54
22-26	800	2.4	1.92	2.8	0.59
26-31	400	2	1.67	15.97	3.76

From the hardware study it can be concluded that even though CSS based HOSMC has considerable margin of steady state error and overshooting of RP from the sliding surface resulting in slow settling time. This can be overcome by PID sliding surface which can be tuned to operate in optimum state providing high tracking accuracy while also maintaining faster settling time. A closer look at the responses of the two sliding surfaces has been presented in Fig.16.The reference speed has been changed from 800 RPM to 1200 RPM at t = 13s. The RP moves out of the sliding surface at this point and the control signal is continuous until the RP moves back onto the sliding surface. The PIDSS HOSMC pulls the RP back on to the sliding surface at t = 14s. On inspecting the control signal of CSS HOSMC, it can be noticed that RP moves towards the sliding surface and the CSS HOSMC fails to latch the RP onto the surface and RP traverses away from the sliding surface and is then pulled back on to the surface at t = 14.4s.

Table 7 and Fig.15 and Fig.16 make it evident that the speed of CSS second order SMC has comparatively poor response time to changes in reference speed. The response of PIDSS second order SMC has high tracking accuracy and faster settling time. From the Table 4 and Table 7 the average error margin between simulation and hardware results for CSS and PIDSS controllers is calculated as follows:

Table 8. Average Error % (Simulation vs Hardware)

Controller	Average Error % (Simulation)	Average Error % (Hardware)	Mean Deviation (%)
CSS	3.34	5.65	2.31
PIDSS	0.97	1.36	0.39

6. Conclusion

This paper presents a thorough design, simulation analysis and hardware implementation of Higher Order Sliding Mode Control for Buck-Boost Converter fed PMDC motor. The controller was modelled from the regularized set of equations, simulated in MATLAB/Simulink for changing load torque conditions and then implemented in real-time with Arduino UNO controller for no-load condition. The PIDSS is compared with CSS and it is proved that PIDSS had shown better effectiveness in regulation of speed, reduces chattering and quicker response time. This work constructs a second order sliding mode control for a buck-boost converter fed PMDC motor and presents simulation results from MATLAB/Simulink for changing load torques and hardware results under no-load condition. Furthermore, the present work will be extended in the future to include hardware implementation under various loaded conditions. In addition, the proposed control method can be further explored for broader real-world applications such as electric vehicles, robotic actuators, and renewable energy integration systems, where high precision and robustness are essential.

7. Acknowledgment

The authors acknowledge the Department of Electrical and Electronics Engineering, Anna University as well as the RUSA 2.0 (PO 2) project for their financial support.

8. References

[1]. Fazdi MF, Hsueh P-W. Parameters Identification of a Permanent Magnet DC Motor: A Review. *Electronics*. 2023; 12(12):2559. https://doi.org/10.3390/electronics12122559

[2]. H. Gaied, A. Flah, H. Kraiem and L. Prokop, "A Comparison Between the Quality of Two Level and Three Levels Bidirectional Buck-Boost Converter Using the Neural Network Controller," in *IEEE Access*, vol. 12, pp. 94323-94336, 2024, doi: 10.1109/ACCESS.2024.3403769.

[3]. M. Dasohari, N. Vishwanathan, S. Porpandiselvi and A. R. M. Vani, "A Soft-Switched Boost Converter Based LED Driver With Reduced Input Current Ripple," in *IEEE Access*, vol. 12, pp. 45904-45922, 2024, doi: 10.1109/ACCESS.2024.3377122.

[4]. B. Ullah, H. Ullah and S. Khalid, "Direct Model Predictive Control of Noninverting Buck-boost DC-DC Converter," in *CES Transactions on Electrical Machines and Systems*, vol. 6, no. 3, pp. 332-339, September 2022, doi: 10.30941/CESTEMS.2022.00043.

[5]. Sarah K. Spurgeon, “Sliding mode control: a tutorial”, European Control Conference (ECC 2014), 25-27 June 2014, Strasbourg, France.

[6]. Jianping Guo,A novel high order sliding mode control method,ISA Transactions,Volume 111,2021,Pages 1-7,ISSN 0019-0578,https://doi.org/10.1016/j.isatra.2020.11.015.

[7]. Arie Levant, “Homogeneity approach to high-order sliding mode design”, Automatica Volume 41, Issue 5, May 2005, Pages 823-830

[8]. Vadim Utkin, “Discussion Aspects of High-Order Sliding Mode Control”, *IEEE Transactions On Automatic Control*, Vol. 61, No. 3, March 2016.
[9]. Damiano A, Gatto G.L, Marongiu I and Pisano A, “Second-Order Sliding-Mode Control of DC Drives”, *IEEE Transactions on Industrial Electronics* (Volume: 51, Issue: 2, April 2004)
[10]. Dhanasekar Ravikumar and Ganesh Kumar Srinivasan, “Implementation of higher order sliding mode control of DC–DC buck converter fed permanent magnet DC motor with improved performance”, *Automatika-Journal for Control, Measurement, Electronics, Computing and Communications* Volume 64, 2023 - Issue 1
[11]. Luan M, Ruan J, Zhang Y, Yan H, Wang L. An Improved Adaptive Finite-Time Super-Twisting Sliding Mode Observer for the Sensorless Control of Permanent Magnet Synchronous Motors. *Actuators*. 2024; 13(10):395. https://doi.org/10.3390/act13100395
[12]. D. Ravikumar, G. K. Srinivasan and M. Rivera, "Performance enhancement of permanent magnet DC motor with sepic converter through higher order sliding surface," in *IEEE Latin America Transactions*, vol. 22, no. 9, pp. 789-797, Sept. 2024, doi: 10.1109/TLA.2024.10670234.
[13]. R, D., Srinivasan, G.K. and Rivera, M. (2024), "A novel higher-order sliding mode control for DC-DC boost converter system in PMDC motor exploring mismatched disturbances", *Circuit World*, Vol. 50 No. 2/3, pp. 348-364. https://doi.org/10.1108/CW-06-2023-0144
[14]. Afifa R, Ali S, Pervaiz M, Iqbal J. Adaptive Backstepping Integral Sliding Mode Control of a MIMO Separately Excited DC Motor. *Robotics*. 2023; 12(4):105. https://doi.org/10.3390/robotics12040105
[15]. Orta-Quintana ÁA, García-Chávez RE, Silva-Ortigoza R, Marciano-Melchor M, Villarreal-Cervantes MG, García-Sánchez JR, García-Cortés R, Silva-Ortigoza G. Sensorless Tracking Control Based on Sliding Mode for the “Full-Bridge Buck Inverter–DC Motor” System Fed by PV Panel. *Sustainability*. 2023; 15(13):9858. https://doi.org/10.3390/su15139858
[16]. Velasco-Muñoz H, Candelo-Becerra JE, Hoyos FE, Rincón A. Speed Regulation of a Permanent Magnet DC Motor with Sliding Mode Control Based on Washout Filter. *Symmetry*. 2022; 14(4):728. https://doi.org/10.3390/sym14040728.
[17]. Chamundeeswari, V., & Seyezhai, R. (2023). Design and Implementation of Fuzzy sliding mode control (FSMC) approach for a Modified Negative Output Luo DC-DC Converter with its comparative analysis. Automatika, 65(1), 45–57. https://doi.org/10.1080/00051144.2023.2280875
[18]. A. Sferlazza et al., "Nonlinear Robust Control of a Differential Boost Inverter Based on Disturbance Compensation and Additional Sliding-Mode Component," in IEEE Access, vol. 12, pp. 98634-98646, 2024, doi: 10.1109/ACCESS.2024.3427671.
[19]. J. Fei and X. Gong, "Self-Organizing Fuzzy Neural Nonsingular Fast Terminal Sliding Mode Control of DC-DC Buck Converter," in *IEEE Transactions on Circuits and Systems I: Regular Papers*, vol. 71, no. 9, pp. 4309-4322, Sept. 2024, doi: 10.1109/TCSI.2024.3416462.
[20]. J. Fei and D. Jiang, "Fuzzy Neural Network Sliding-Mode Controller for DC-DC Buck Converter," in *IEEE Internet of Things Journal*, vol. 11, no. 19, pp. 31575-31586, 1 Oct.1, 2024, doi: 10.1109/JIOT.2024.3418492.
[21]. G. Rinaldi, P. P. Menon and A. Ferrara, "Design and Experimental Validation of an Embedded Sliding Mode Controller for Voltage Regulation With SEPIC Converters," in *IEEE Transactions on Power Electronics*, vol. 39, no. 9, pp. 11034-11046, Sept. 2024, doi: 10.1109/TPEL.2024.3415164.
[22]. Gudey SK, Malla M, Jasthi K, Gampa SR. Direct Torque Control of an Induction Motor Using Fractional-Order Sliding Mode Control Technique for Quick Response and Reduced Torque Ripple. *World Electric Vehicle Journal*. 2023; 14(6):137. https://doi.org/10.3390/wevj14060137

[23]. Maidana P, Medina C, Rodas J, Maqueda E, Gregor R, Wheeler P. Sliding-Mode Current Control with Exponential Reaching Law for a Three-Phase Induction Machine Fed by a Direct Matrix Converter. *Energies*. 2022; 15(22):8379. https://doi.org/10.3390/en15228379

[24]. F. Noor, K. Zeb, S. Ullah, Z. Ullah, M. Khalid and A. Al-Durra, "Design and Validation of Adaptive Barrier Function Sliding Mode Controller for a Novel Multisource Hybrid Energy Storage System Based Electric Vehicle," in *IEEE Access*, vol. 12, pp. 145270-145285, 2024, doi: 10.1109/ACCESS.2024.3471893.

[25]. Deepa, B. R., & Linda, M. M. (2024). Analysis of single phase ZSI fed PV system in weak grids using fractional order sliding mode control technique. Automatika, 65(3), 830–841. https://doi.org/10.1080/00051144.2024.2314903

[26]. Komurcugil H, Biricik S, Bayhan S, et al. Sliding mode control: overview of its applications in power converters. *IEEE Ind Electron Mag*. March 2021;15(1):40–49. DOI:10.1109/MIE.2020.2986165

Dhanasekar Ravikumar (Senior Member in IEEE) is currently working as an Associate Professor in the Department of Electrical and Electronics Engineering at Sri Sairam Institute of Technology, Chennai, India. He has served as a reviewer for international journals, including IEEE Latin America Transactions, Electric Power Components and Systems, Journal of Dynamic Systems, Measurement and Control, and Scientific Reports. He graduated with a degree in Electrical and Electronics Engineering from RVS College of Engineering & Technology, Tamilnadu, India, in 2004, earned his Master's in Power Electronics & Drives from Mepco Schlenk Engineering College, Tamilnadu, India, in 2006, and completed his PhD at CEG, Anna University, Chennai, Tamilnadu, India.

Vijayaraja Loganathan (Member in IEEE) was born on May 30, 1983 and in 2023 from Anna University in Chennai, India, where he earned his Ph.D. He is currently employed by Sri Sairam Institute of Technology in Chennai, India, as an Associate Professor. Electric vehicles, power converter and inverter designs, renewable energy sources are among his research interests. More than 60 of his research papers have been published in academic journals, conferences held abroad, and technical book series. Also, he has more than 5 patents and 2 patent grants in his area of study.

Ganesh Kumar Srinivasan (Member in IEEE) is presently working as Professor in the Department of EEE, College of Engineering Guindy, Anna University, Chennai, India. He actively involved in the field of multilevel inverters and control of power converters. He has published 29 journals, 32 conference papers and 3 patents. He have completed two research projects with Rs 27 Lakhs and presently doing two projects of worth Rs 3 Crores.

Arman Salih Ahmad A was born on July 20, 1999. He obtained his Bachelor of Engineering (B.E.) in Electrical and Electronics Engineering (EEE) from M.I.E.T Engineering College, Trichy, in 2016, followed by a Master of Engineering (M.E.) in Power Electronics & Drives from College of Engineering, Guindy, Anna University, Chennai, in 2023. From 2023 to 2024, he worked as a Product Specialist (Low-Frequency Electromagnetics) at Altair, Chennai. Currently, he is pursuing a Ph.D. degree in Electrical Engineering at IIT Madras.